

A PARAMETRIC STUDY OF THE AIR FLOW IN AN ELECTRIC GENERATOR THROUGH STEPWISE GEOMETRY MODIFICATIONS

Piروز Moradnia and Håkan Nilsson

Chalmers University of Technology,
412 96 Gothenburg, Sweden
e-mail: {piروز.moradnia,hakan.nilsson}@chalmers.se

Key words: Fluid Dynamics, CFD, Generator, Air Flow

Abstract. *The air flow through an electric generator has been numerically investigated to give a better understanding of the flow for cooling purposes. A simple generator design has been chosen to start with, and stepwise modifications have been imposed to the design of the rotor and the stator. The flow properties for all cases have been compared to each other to investigate the effect of each parameter change on the flow inside the machine.*

The flow is predicted with the OpenFOAM solver MRFSimpleFOAM, which is a steady-state solver that uses the Frozen Rotor concept for the rotor-stator interaction. This means that there is no actual mesh movement in this study, but instead, the rotating regions in the domain are provided with source terms that account for rotation. The flow through the machine is not explicitly specified. Instead, it is the effect of the rotating regions that drive the flow through the machine. The reason for this is the lack of knowledge of the flow rate and inlet velocity distribution, which requires an approach without inlet and outlet. The flow is thus recirculating in the computational domain.

1 INTRODUCTION

Almost half of the total electric power generation in Sweden comes from the hydroelectric power plants. Obviously any modifications and improvements to these systems would lead to considerable contributions to the total electric energy produced in the country. As any other complicated system, a hydroelectric power plant comprises a large number of different components, any of which should be carefully designed and optimized with respect to the working conditions to yield the highest possible efficiency at the normal working conditions.

In this work, the focus is on electric generators and the cooling air flow within them. A generator is a device which generates electricity through magnetic induction into its coils. The generator is made up of two main components: a rotor and a stator. The rotor is the rotating part of the generator, which holds a number of large electromagnetic poles. The stator is the stationary part, which is composed of a large number of electric conductors, called windings. When the rotor rotates, the motion of its magnetic field induces an alternating electric current in the stator windings. A transformer is then used to increase the voltage which leads to a decreased current with the same power, ($Power = Voltage \times Current$). The electricity is then transmitted to the network.

The process of conversion of the mechanical energy into electricity includes losses due to electrical resistance, magnetic field, and mechanical losses. The losses rise the temperature of the components, which leads to a change in the material properties. This includes electric resistances and conductivities, which are temperature dependent. A working temperature beyond the prescribed values may result in deteriorated performance and lower efficiency of the generator in converting the energy to electricity. Also, the material strengths of certain components, such as insulations, are affected by temperature, causing a reduction in life time. All this means that the heat generated by the energy conversion process in the generators should be removed in order to keep the machine near its best operational point. Usually the heat in a generator is removed by means of convection. A number of cooling channels are provided in the stator body to allow for the passage of air to cool down the stator windings. The rotor acts as a fan, which builds up a pressure difference that pushes the air through the stator channels. Figure 1 shows the different parts of an axially cooled generator. In an axially cooled generator, the air flows axially into the machine and passes through the space between the rotor poles and into the stator channels. The stator channels are extended radially through the stator.

The aim of this work is to numerically study the air flow in an axially cooled generator. Heat transfer is not included in the present study. The effect of adding stator baffles and rotor fan blades on the cooling air flow in a generator has been investigated in a previous work¹. This work extends the studies by considering the effect of different rotor pole designs on the air flow inside a generator. The numerical computations have been performed using the OpenFOAM solver MRFSimpleFOAM, and the choice of the turbulence model has been based on a detailed study of the turbulence models in OpenFOAM².

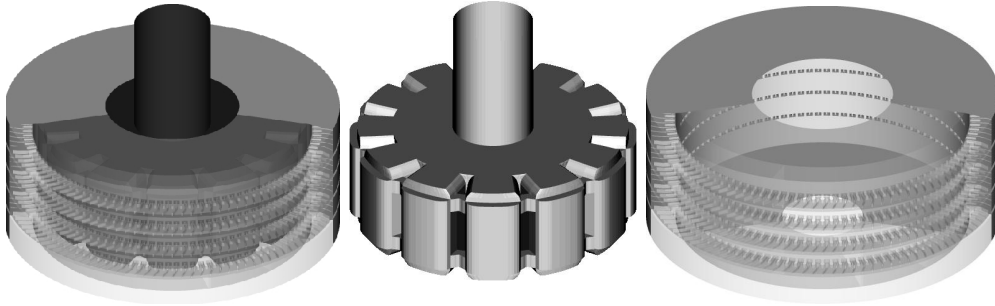


Figure 1: The simplified generator geometry used in the present work. Left: the complete model. Center: the rotor. Right: the stator. Transparency has been used to visualize the interior of the geometry.

2 CASE SETUPS

As Figure 1 shows, the rotor in the present study has 12 poles. The stator body contains a number of air passages, called stator channels, which allow for the flow of the cooling air through the generator. Figure 2 shows the stator channels and their relative positions to the rotor pole in the present Frozen-Rotor set-up. The stator channels are separated in the tangential direction by small baffles, which are used as supports to separate the stator plates. A stator winding passes through each channel between the baffles.

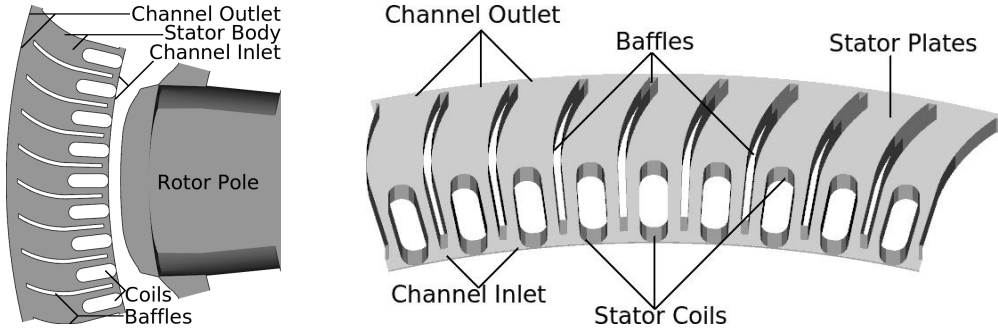


Figure 2: Left: The rotor pole and the stator channels viewed from above. Right: A close-up view of the stator channels.

The channels are provided in 4 axial rows. Each row contains 108 channels. With 108 stator channels in each row, each pole can be associated with 9 channels in the circumferential direction. Thus, one can simplify the problem by modeling only 1 pole with 9 corresponding channels in each row, i.e. only a 1/12 sector with periodic boundaries. Also, since the geometry is axially symmetric, the computational domain can be further reduced by considering only the upper part and utilizing a symmetry boundary condition at the symmetry plane.

Figure 3 shows the computational domain by visualizing all the boundaries except the periodic boundaries of one of the studied cases, and a cross-section of the pole and the nine stator channels with their coils and baffles. The position for sampling the volume flow distributions is selected to be at the backside of the coils and is shown in Figure 3.

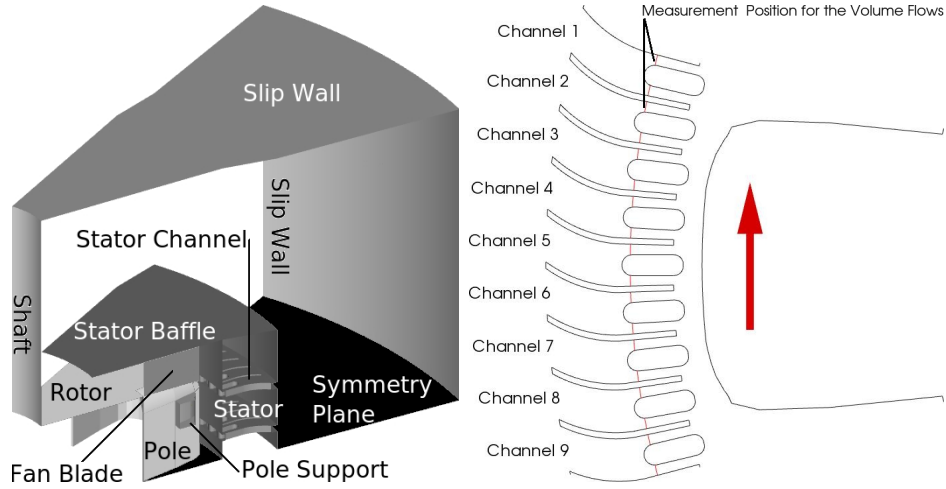


Figure 3: Left: Computational domain where the 1/12 periodic sector and symmetry plane can be seen. The front and back boundaries (not shown) are periodic. Right: Rotor pole and stator cooling channels. The rotor is moving clockwise when seen from above.

The computational domain is generated without inlets and outlets. It is thus the rotation of the rotor which drives the flow, and the volume flow through the machine is determined by the solution rather than by a prescribed value at an inlet. The flow is recirculating through the inclusion of a large surrounding

The flow is driven by the pressure build-up caused by the rotation of the rotor and interaction of the air flow with the rotor and stator walls. Noticing the movement of the rotor relative to the stator, the flow should be pulsating and unsteady. In the present work, however, the simulations have been performed using the steady-state Frozen Rotor concept. In the Frozen Rotor concept the computational domain and the corresponding mesh are not rotating, but instead source terms for the rotation have been added to the governing equations in the rotating region. The Navier-Stokes and continuity equations then read³

$$\begin{aligned} \nabla \cdot (\vec{u}_R \otimes \vec{u}_I) + \vec{\Omega} \times \vec{u}_I &= -\nabla(p/\rho) + \nu \nabla \cdot \nabla(\vec{u}_I) \\ \nabla \cdot \vec{u}_I &= 0 \end{aligned} \quad (1)$$

where \vec{u}_I is the velocity in the inertial reference frame, \vec{u}_R is the velocity in the rotating frame of reference and $\vec{\Omega}$ is the rotation vector of the rotating frame of reference.

The turbulence is modeled utilizing the low-Re Launder-Sharma turbulence model⁴. The choice of the turbulence model was based on a detailed study of the turbulence models in OpenFOAM². The use of a low-Re turbulence model is justified by the relatively small Reynolds numbers in the stator channels. It is beneficial with a fine mesh to capture the sharp gradients, especially in the near-wall regions where the modeled wall shear stresses are quite sensitive to the mesh quality. A high-Re turbulence model would lead to a mesh that is too coarse to resolve many of the flow features. The k and ε equations in the Launder-Sharma model read

$$\begin{aligned} \frac{Dk}{Dt} &= \frac{\partial}{\partial x_j} \left[\left(\nu + \frac{\nu_t}{\sigma_k} \right) \frac{\partial k}{\partial x_j} \right] + P_k - \tilde{\varepsilon} - D \\ \frac{D\tilde{\varepsilon}}{Dt} &= \frac{\partial}{\partial x_j} \left[\left(\nu + \frac{\nu_t}{\sigma_\varepsilon} \right) \frac{\partial \tilde{\varepsilon}}{\partial x_j} \right] + C_{\varepsilon 1} f_1 \frac{\tilde{\varepsilon}}{k} P_k - C_{\varepsilon 2} f_2 \frac{\tilde{\varepsilon}^2}{k} + E \end{aligned} \quad (2)$$

$\tilde{\varepsilon}$	D	E	f_μ	f_1	f_2
$\varepsilon - D$	$2\nu \left(\frac{\partial \sqrt{k}}{\partial x_j} \right)^2$	$2\nu \nu_t \left(\frac{\partial^2 U_i}{\partial x_j \partial x_k} \right)^2$	$e^{\left(\frac{-3.4}{(1+R_T/50)^2} \right)}$	1	$1 - 0.3e^{(-R_T^2)}$
R_T	c_μ	$c_{\varepsilon 1}$	$c_{\varepsilon 2}$	σ_k	σ_ε
$\left(\frac{k^2}{\nu \tilde{\varepsilon}} \right)$	0.09	1.44	0.92	1.0	1.22

3 CASES AND RESULTS

The geometry is a simplified version of a small generator at Uppsala University in Sweden. A parametric study of the effect of different parts of the geometry on the flow has been performed. Table 1 shows the specifications of all the different cases that have been studied in the present work.

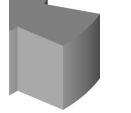
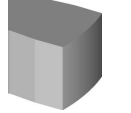
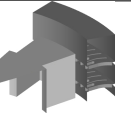
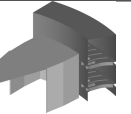
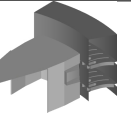
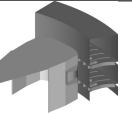
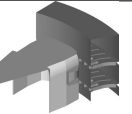
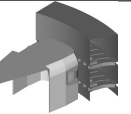
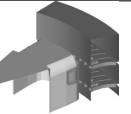
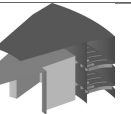
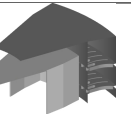
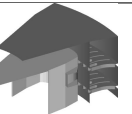
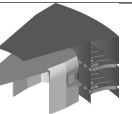
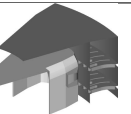
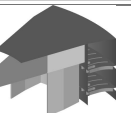
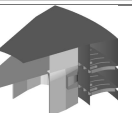
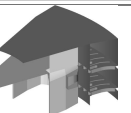
#	1	2	3	4	5	6	7
<i>Pole</i>							
<i>C#</i>							
<i>C#S</i>							
<i>C#F</i>							
A_1	$0.0033m^2$	$0.0029m^2$	$0.0029m^2$	$0.0029m^2$	$0.0029m^2$	$0.0029m^2$	$0.0028m^2$
A_2	$0.0028m^2$	$0.0017m^2$	$0.0017m^2$	$0.0017m^2$	$0.0017m^2$	$0.0017m^2$	$0.0017m^2$

Table 1: Different rotor and stator designs. A_1 is the cross-sectional area between the poles. A_2 is the cross-sectional area of the air gap between the rotor and the stator.

A simple pole design was selected and then modified in several steps to resemble the real geometry at the end. The generator cases include modifications to the rotor pole and the stator. There are 7 different rotor pole designs. Each pole design is assigned a number (from 1 to 7). Except for the pole design 1, each pole design is based on the previous pole design with geometric modifications. Every modified rotor geometry has been simulated with three different layouts: a base case ($C\#$ cases), a case with a baffle on top of the stator ($C\#S$ cases), and a case with a combination of a stator baffle and a rotor fan blade between the poles ($C\#F$ cases). In all cases the stator inner diameter is $0.365m$ and the rotor rotational speed is $500rpm$. Table 2 presents the pole designs and the respective modifications to them. Pictures of the pole designs can be found at the top row of Table 1. Definitions of areas A_1 and A_2 can be seen in Figure 4

Pole design	Remarks and Modifications
1	Base pole geometry with radial pole sides
2	Reduced areas A_1 and A_2 and non-radial sides
3	Added wedge shaped pole supports in between the poles
4	Curved front part of the poles
5	Curved edges on top of the poles
6	More curvature on top of the poles
7	Flattened top-front part of the poles

Table 2: Different rotor pole designs and the respective modifications.

Figure 4 shows the schematic views of A_1 and A_2 as the shaded areas between the rotor and stator. A_1 is the cross-sectional area of the free space between the poles in the symmetry plane in the computational domain. A_2 is the cross-sectional area of the air gap between the rotor and the stator in the symmetry plane in the computational domain.

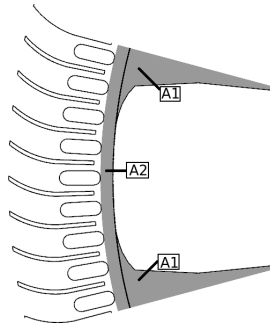


Figure 4: A view of areas A_1 and A_2

3.1 Volume Flow Distributions

The distribution of volume flow between the channels is shown in Figure 5. The volume flow distributions are taken along the curve at the backside of the stator coils as shown

in Figure 3. Each diagram corresponds to one rotor design ($C\#$ variants). The upper diagrams show the upper channel row, and the lower diagrams show the lower channel row. The vertical axis shows the volume flow of each channel. The horizontal axis shows the channel numbers, which are in accordance with the numbering shown in Figure 3, meaning that the rotor is rotating from channel 9 towards channel 1. The vertical dotted lines show the tangential position of the pole edges in relation to the stator channels.

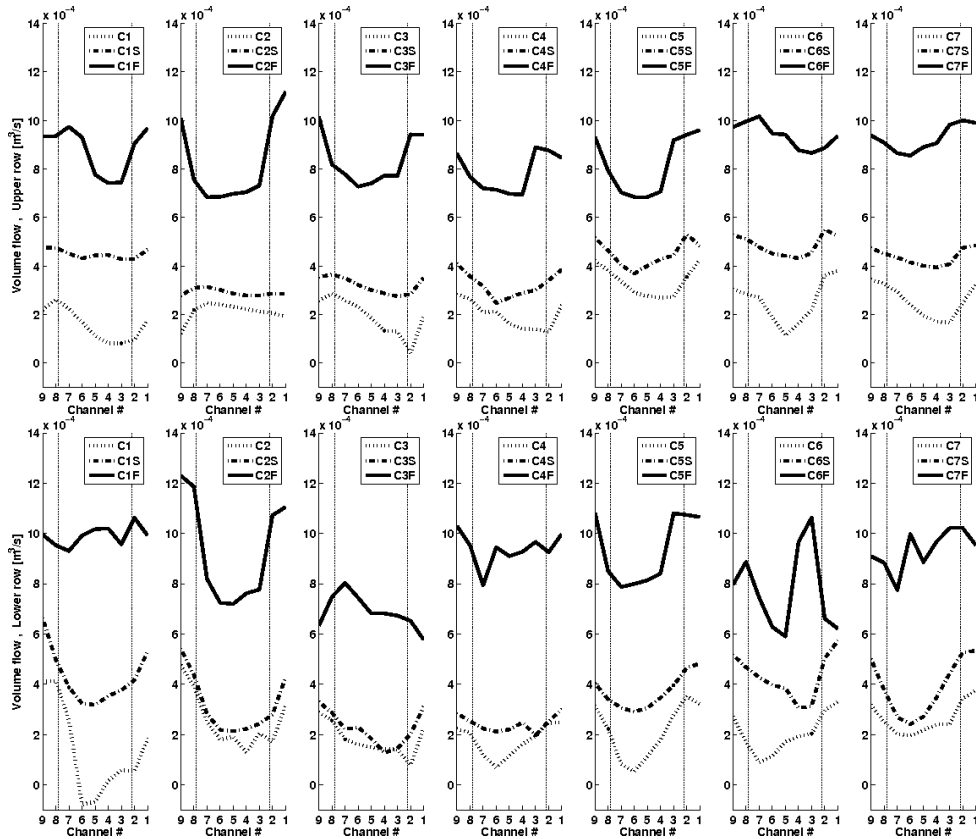


Figure 5: Volume flow distributions in the stator channels. Top: the upper row, bottom: the lower row. From left to right: C1, C2, C3, C4, C5, C6 and C7 variants. Channel numberings according to Figure 3

As Figure 5 suggests, the use of a stator baffle above the rotor ($C\#S$) increases the volume flow through the machine. This is due to the higher pressure build-up inside the machine. Also, the addition of fan blades to the rotor increases the volume flow even more. The increase in volume flow due to the inclusion of fan blades can again be justified by a higher pressure build-up in the generator. A larger pressure difference between the inside and the outside of the machine leads to a larger volume flow.

Figure 6 shows the relative distribution of the volume flow between the channels for all cases. The small rectangles show the channels in two rows and the large rectangle shows the pole edges. The vertical axis shows the channel volume flow normalized by the total volume flow of each case. The zero- volume flow lines are shown by the horizontal dotted

lines along the center of the channels. In most cases (as will be shown later, the cases without fan blades) the air enters the channel from both sides of the stator windings, while in some cases (as will be shown later, the cases with fan blades) the flow enters the channel from the left side of the winding and some part of the flow exits the channel from the right side of the windings. Notice one case (C1) has a purely negative flow in a channel in the lower row (channel number 6), which means that the flow exits from both sides of the windings in the channel.

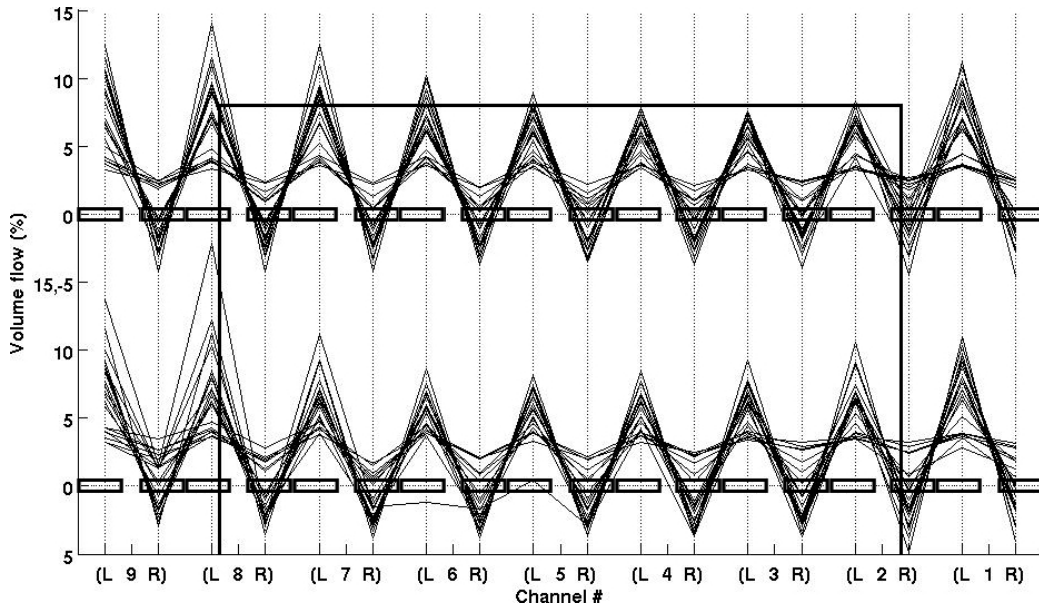


Figure 6: Relative volume flow distribution in all channels. Channel numbering according to Figure 3

Table 3 shows the volume flow in the computational domain, and the average air flow velocity at the minimum cross-sectional area of the stator channels. This local average velocity is computed by dividing the volume flow through the computational domain by the minimum cross-sectional area of the stator channels by the number of the stator channels included in the computational domain. The minimum cross-sectional area of a single stator channel, near the stator coils, is $A_m \approx 8.29 \times 10^{-5} (m^2)$. It should be noted that each case has its own volume flow, \dot{V}_f , which is obtained by the solution. Since a total number of 18 stator channels are included in the computational domain, the average velocity at the minimum cross-sectional area is given by

$$v_m = \frac{\dot{V}_f}{18 \times A_m} \quad (3)$$

Table 3 suggests that the volume flow \dot{V}_f , and thus the velocity v_m are smallest for the cases without stator baffles, while adding stator baffles leads to an increased volume flow and thus increases the velocity v_m . The largest volume flows are obtained by combining the stator baffles and rotor fan blades.

<i>Pole#</i>		C1	C2	C3	C4	C5	C6	C7
<i>C#</i>	$\dot{V}_f(\frac{m^3}{s})$	0.0027	0.0042	0.0033	0.0034	0.0050	0.0041	0.0047
	$v_m(\frac{m}{s})$	1.8	2.8	2.2	2.3	3.3	2.8	3.1
<i>C#S</i>	$\dot{V}_f(\frac{m^3}{s})$	0.0079	0.0055	0.0049	0.0051	0.0074	0.0083	0.0075
	$v_m(\frac{m}{s})$	5.3	3.7	3.3	3.4	5.0	5.5	5.0
<i>C#F</i>	$\dot{V}_f(\frac{m^3}{s})$	0.0168	0.0158	0.0137	0.0155	0.0157	0.0154	0.0168
	$v_m(\frac{m}{s})$	11.2	10.6	9.2	10.4	10.5	10.3	11.2

Table 3: Rotor pole design, volume flow and average stator channel flow velocity. $\dot{V}_f(\frac{m^3}{s})$: The volume flow rate through the computational domain, $v_m(\frac{m}{s})$: Average velocity at the minimum channel cross-sectional area

3.2 Rotor Axial Power

The axial power of the rotor is divided into two parts⁵: a part to overcome the moments from pressure forces, \dot{E}_p , and a part to overcome the moments from viscous forces, \dot{E}_v . The total power is then found by summing the two parts: $\dot{E}_{rotor} = \dot{E}_p + \dot{E}_v$. Table 4 shows the respective powers for all cases.

<i>Pole#</i>		C1	C2	C3	C4	C5	C6	C7
<i>C#</i>	$\dot{E}_p(W)$	4.45	2.42	2.24	2.27	4.04	3.73	3.13
	$\dot{E}_v(W)$	0.30	0.34	0.34	0.32	0.28	0.23	0.24
<i>C#S</i>	$\dot{E}_p(W)$	3.62	2.29	1.94	1.98	2.82	3.25	2.94
	$\dot{E}_v(W)$	0.25	0.31	0.28	0.28	0.26	0.26	0.24
<i>C#F</i>	$\dot{E}_p(W)$	7.07	7.59	6.00	6.01	5.97	6.30	6.50
	$\dot{E}_v(W)$	0.24	0.11	0.19	0.22	0.23	0.25	0.23

Table 4: Rotor axial power for all cases. $\dot{E}_p(W)$: The axial power required on the rotor to overcome the pressure moments. $\dot{E}_v(W)$: The axial power required on the rotor to overcome the frictional moments.

As Table 4 suggests, the contribution from viscous forces is much smaller than that of the pressure forces. Large separation regions lead to large pressure drops on the rotor pole surfaces which exert large forces on the pole in the direction opposite to the motion of the rotor. The use of a stator baffle leads to a reduction in \dot{E}_p and generally a small reduction in \dot{E}_v . The use of fan blades strongly increases \dot{E}_p but still reduces \dot{E}_v . The increase in \dot{E}_p with the use of fan blades can be justified by the larger volume flow through the generator. The amount of air flowing through the machine is larger and the fan blades should give rotation to the flow, which means that more power is needed to rotate the rotor. Also, large separation areas behind the blades lead to a large pressure loss in those regions.

The reduction in \dot{E}_v can be justified by taking into account that using fan blades helps pushing more air in the desired direction within the machine. This means that the recirculations in the vicinity of the pole are minimized and, thus, friction between the

air and the pole is also reduced.

3.3 Flow Between the Rotor Poles

The unit vectors of the velocity between the rotor poles (the cyclic boundaries in the computational domain, c.f. Figure 3) are shown in Table 5.

#	$C\#$	$C\#S$	$C\#F$
1			
2			
3			
4			
5			
6			
7			

Table 5: Velocity unit vectors in a plane between two poles (the periodic boundary, c.f. Figure 3).

The use of unit vectors makes the flow behaviour more clear in this case, where there is a large difference in velocity magnitudes. The contours of zero axial velocity are marked by thin curves. Ideally, the velocity vectors should not point upwards in the computational domain (upper half of the generator). This means that the flow at the inlet to the machine should always be inwards and that all the fluid should flow directly through the channels. This way the air is heated up by the hot surfaces of the machine and removes the heat by flowing directly outwards. This does not happen in practice, since a number of flow recirculations will appear, based on the design of rotor and stator, as well as the rotational speed of the rotor. The recirculation of the cooling air in the machine causes the air to get warmer as it stays a longer time in contact with the hot surfaces, which reduces

the temperature difference between the surfaces and the cooling air. This impairs the convective cooling of the machine.

In all cases, there is a region near the stator inner wall which has upward velocity vectors. This is not desirable according to the descriptions above. Also, it makes it difficult to define and use appropriate inlet boundary conditions (at the inlet to the machine) which can suit the flow characteristics. This justifies the use of stator baffles which prohibit the outward flow at the inlet to the machine, as the inlet size is reduced and the inlet is moved radially inwards. Obviously, adding a baffle on top of the rotor-stator space forces the velocity vectors to be directed downwards, which increases the inward flow inside the generator. This is based on the negative pressure gradients at the new inlet to the machine, which is stronger than in the base cases.

The fan blades cause an even stronger pressure build-up within the machine, which drives the flow more inwards in the presence of a stator baffle and helps to almost remove the upward-velocity regions inside the generator. This helps minimizing the upward flow near the stator inner wall. The cases with a stator baffle show an obvious separation bubble at the tip of the stator baffle. The separation happens because the fluid flows normal to the baffle at the inlet. However, the separation zone gets smaller in size when the fan blades are introduced. This is because the flow rates are higher with use of fan blades, which is again caused by larger pressure gradients in the domain.

3.4 Flow in the Channels

Tables 6 and 7 show the recirculation zones in the upper and the lower stator channels respectively. The shaded areas show the regions with negative radial velocity. The visualization is made in a plane in the middle of the channel heights. The cases without fan blades show large recirculation regions to the right side of the stator windings, when seen from inside. The cases including fan blades show considerably smaller recirculation areas compared to other cases, and that is mainly visible just behind, or to a small extent, to the right side of the windings. This means that in cases without a fan blade, the air enters the channels from the left side of the stator windings and some part of it exits the channel from the right side of the windings, as previously shown in Figure 6. In the air gap between rotor and stator, separation occurs just to the right side of the stator windings (when seen from inside) and makes a low pressure region there. The low pressure region draws the air from the high pressure region inside the channels, which is undesirable. In cases with fan blades, however, the air enters the channels from both sides of the stator windings. This is caused by the larger pressure build-up inside the machine and leads to a higher flow rate. For the case *C1* the flow in a channel in the lower row has purely negative radial velocities. This means that the fluid flows from the channel into the machine, which is undesirable.

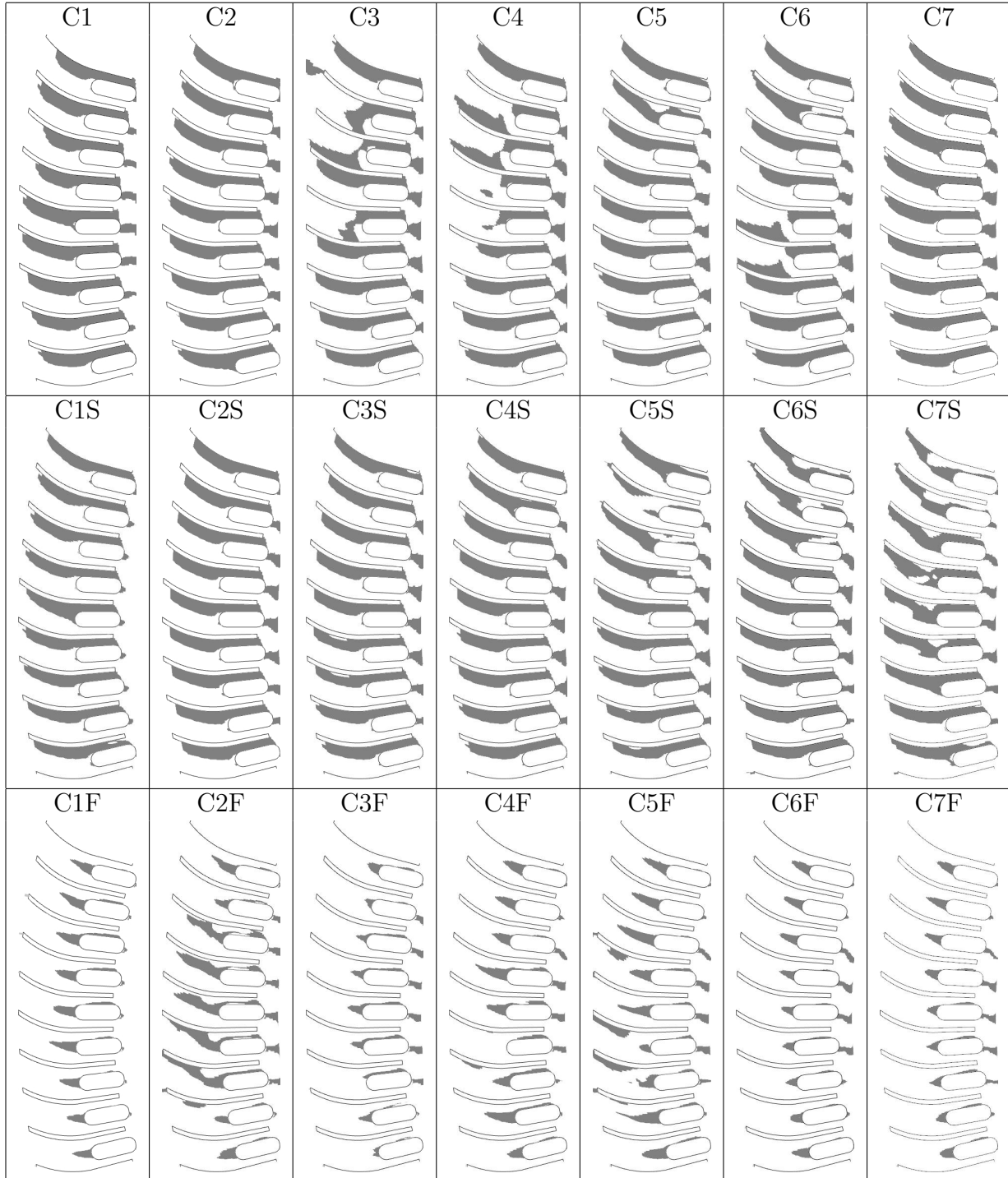


Table 6: Flow in the middle of the upper channel row: The shaded areas show recirculation regions.

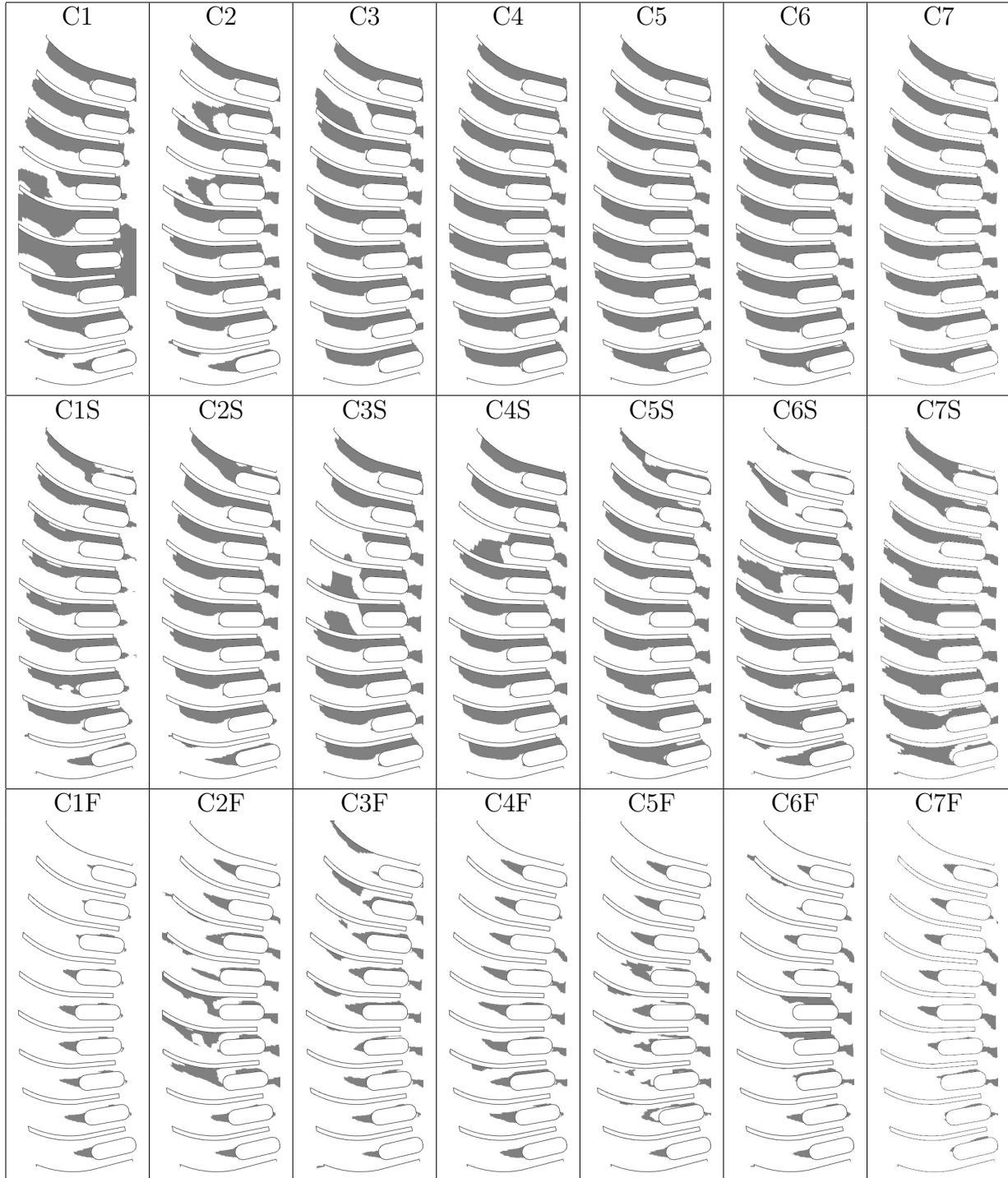


Table 7: Flow in the middle of the lower channel row: The shaded areas show recirculation regions.

3.5 Velocity Components Just Above the Rotor Poles

In tables 8-10 the velocity components are shown in a plane just above the rotor poles. A distance of 0.2mm is chosen between the contours and the pole upper surface.

3.5.1 Axial Velocities

Table 8 shows the axial velocity component just above the rotor poles. A positive sign means that the axial velocity component is directed upwards. In certain cases a region of upward axial velocities are visible, which is not desirable as one would ideally expect inward axial velocities at this location.

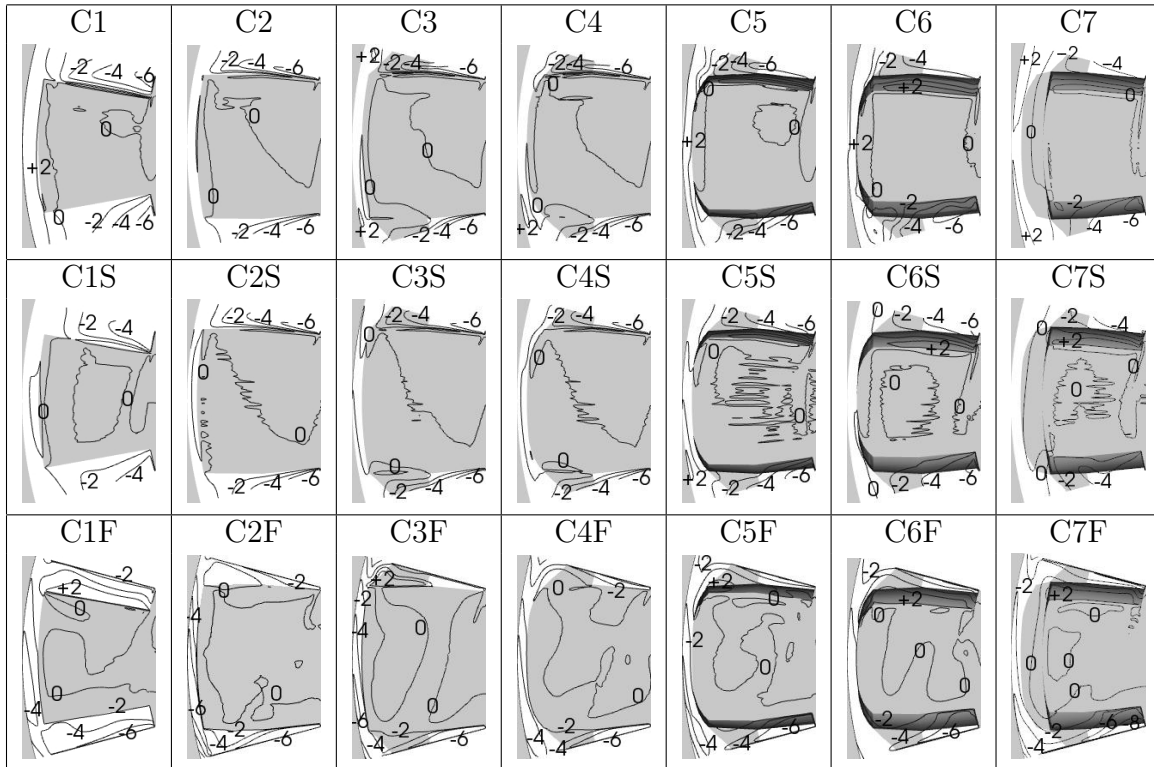


Table 8: Axial velocity just above the rotor poles (m/s)

As Table 8 suggests, the use of stator baffles, as well as the combination of the stator baffles and fan blades on top of the rotor poles, helps decreasing the upward axial velocities and increasing the downward axial velocities in the region between the rotor and the stator. This means that the volume flow inside the machine increases with the use of stator baffles and fan blades.

3.5.2 Tangential Velocities

Table 9 shows the tangential velocity components just above the rotor poles. According to the right-hand rule with rotational axis pointing outward from the pictures, a negative sign means that the rotation takes place clockwise, which in this case means upwards in the pictures. Adding a baffle to the stator increases the average tangential velocity, while the highest tangential velocity is achieved with a fan blade. Rounded pole edges lead to larger tangential velocities just above the rotor.

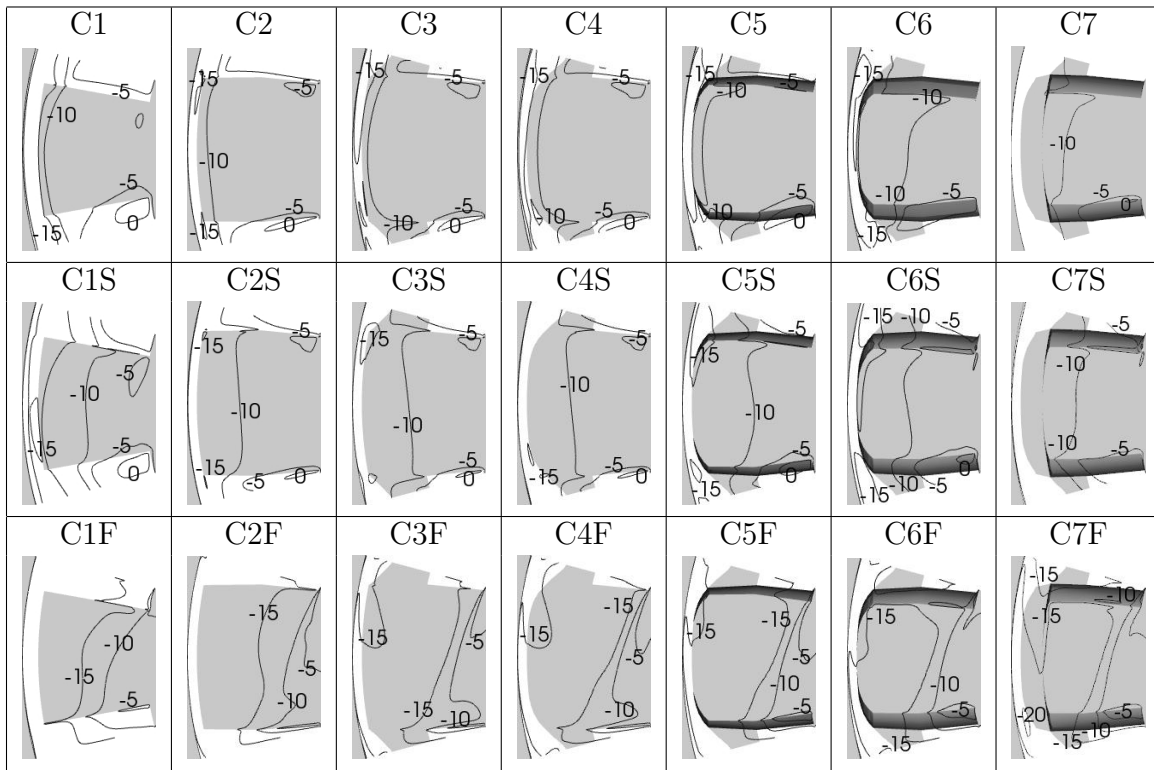
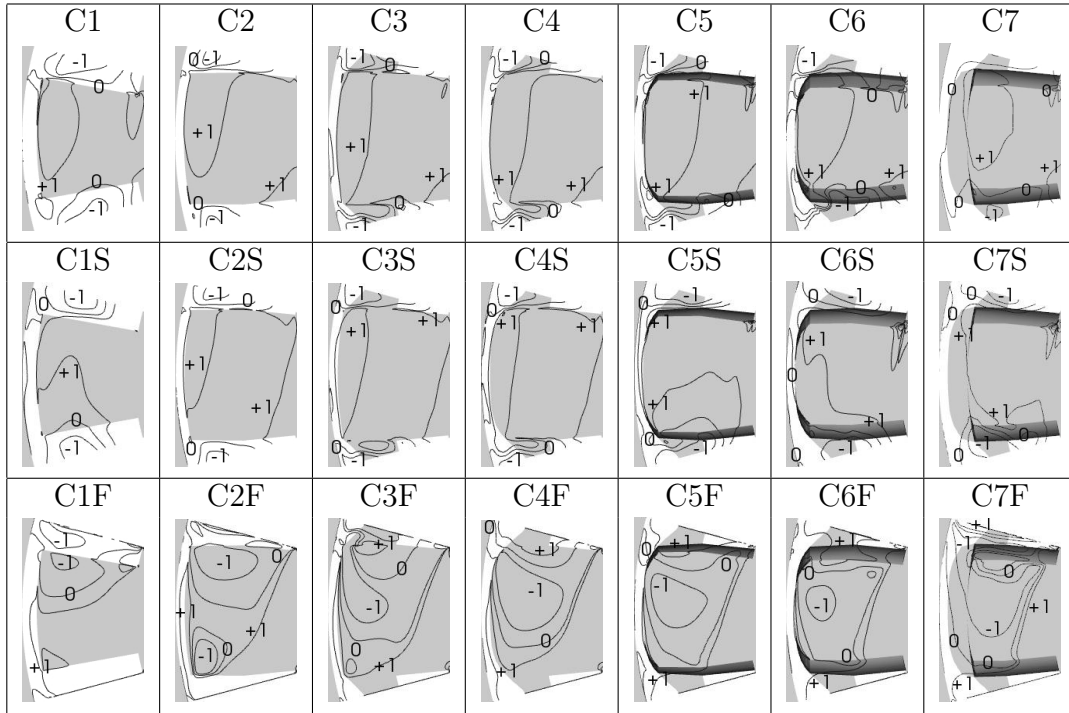


Table 9: Tangential velocity just above the rotor poles (m/s)

3.5.3 Radial Velocities

Table 10 shows the radial velocity component just above the rotor poles. A positive sign means that the velocity is directed radially outwards. In the air gap between the rotor and stator in the cases without a fan blade, there is a region with negative radial velocities, which shows a recirculation between the poles. In the cases with a fan blade, however, the recirculation area is located between the fan blades.


 Table 10: Radial velocity just above the rotor poles (m/s)

3.6 Relative Tangential Velocity in the Pole Gap

The tangential velocity *relative* to the rotor pole is shown in Table 11. The relative component is taken on a plane normal to the axis of rotation and at a height in the middle of the stator channels. The relative velocity component is computed through the relation

$$u_{tangential,relative} = u_{tangential} - \omega r \quad (4)$$

where ωr is the tangential velocity of each point at radius r on the pole. Table 11 suggests that the tangential velocity in the middle of the stator channels is almost the same as the pole tangential velocity, with small differences in certain regions. Near the stator wall the tangential velocity decreases as the fluid gets close to the walls.

3.7 Pressure Distributions on the Rotor Poles

Tables 12, 13, 14 and 15 show the contours of the quantity $\left(\frac{p-p_{ref}}{\rho}\right)$ on the pole top, pole pressure side, pole suction side and pole front. The quantity p refers to the static pressure at each point, while p_{ref} is the static pressure at a reference cell. The reference cell is located just at the top-outer edge of the computational domain. The reference point is, thus, located outside the stator and is identical for all cases. The quantity ρ is the air density.

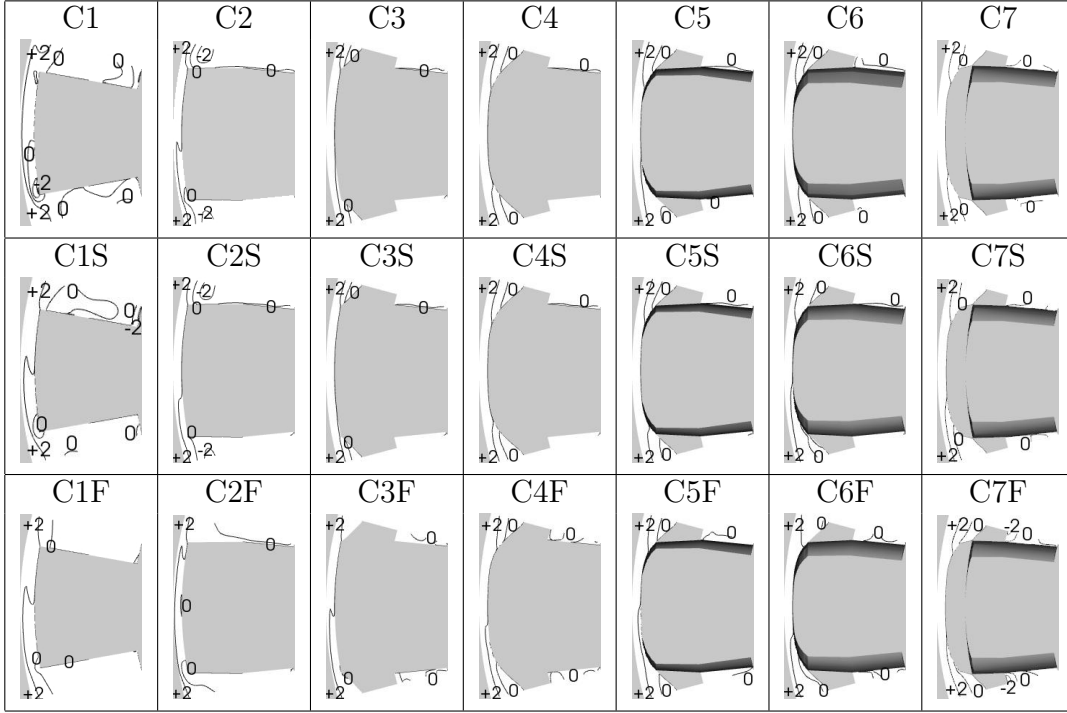


Table 11: Relative tangential velocity, between the stator channels (m/s)

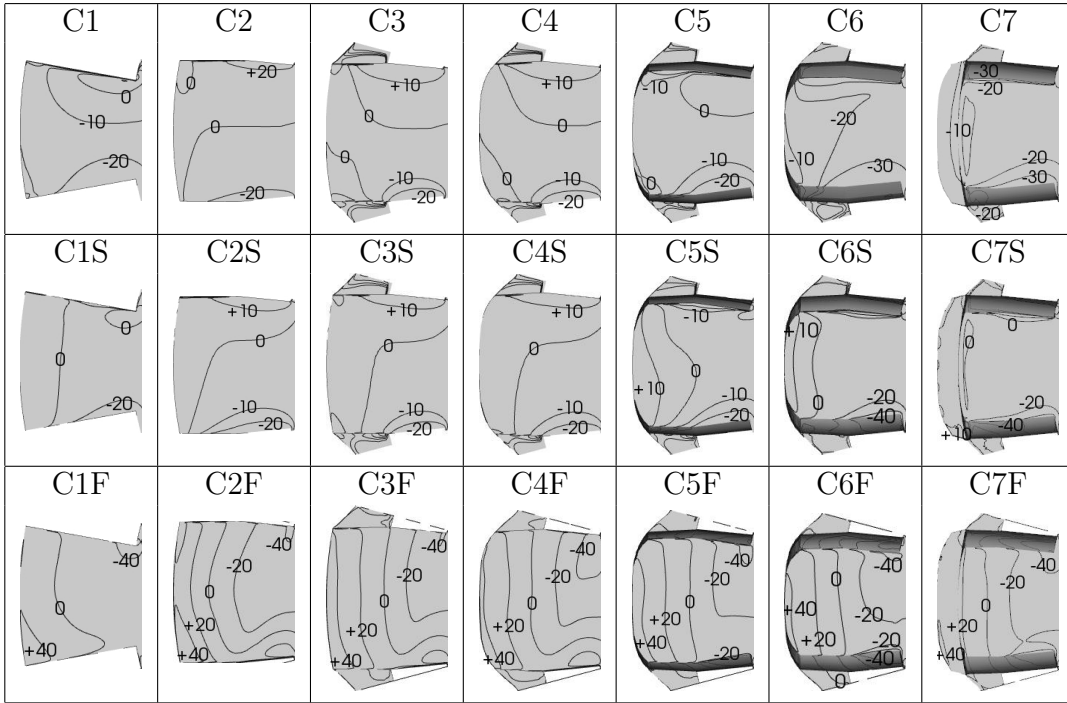


Table 12: Contours of relative static pressure divided by density, $(\frac{p-p_{ref}}{\rho}) [m^2/s^2]$, on the pole top

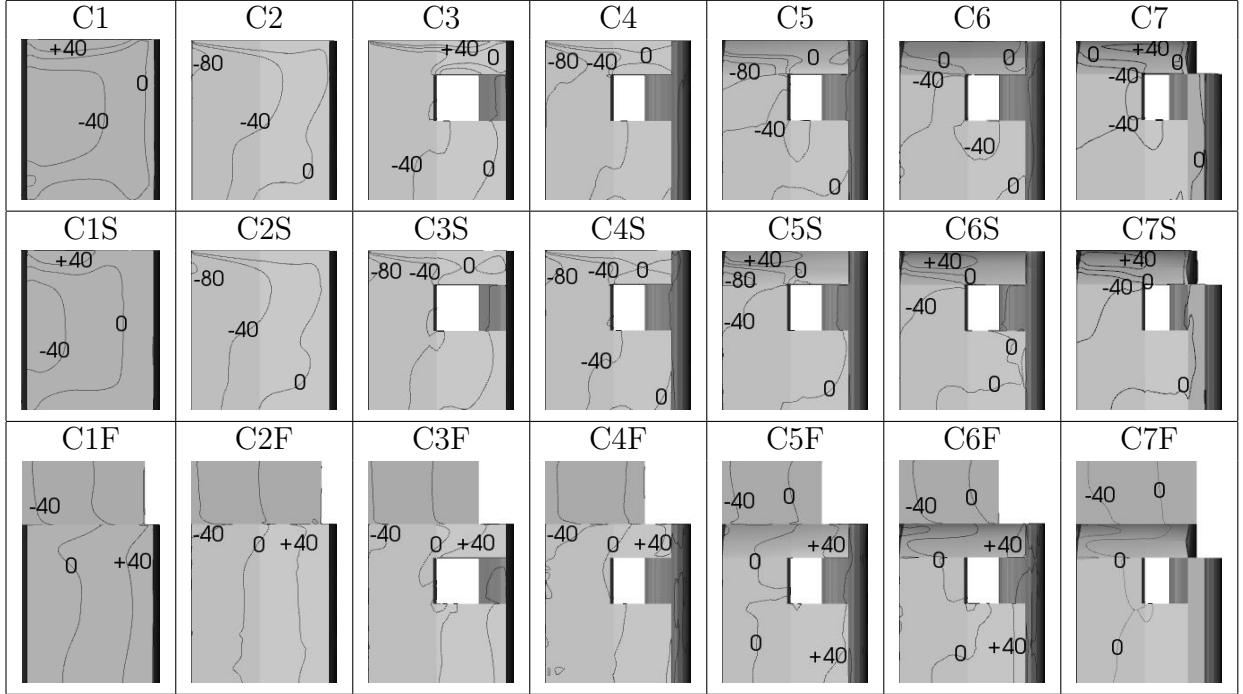


Table 13: Contours of relative static pressure divided by density, $(\frac{p-p_{ref}}{\rho}) [m^2/s^2]$, on the pole pressure side

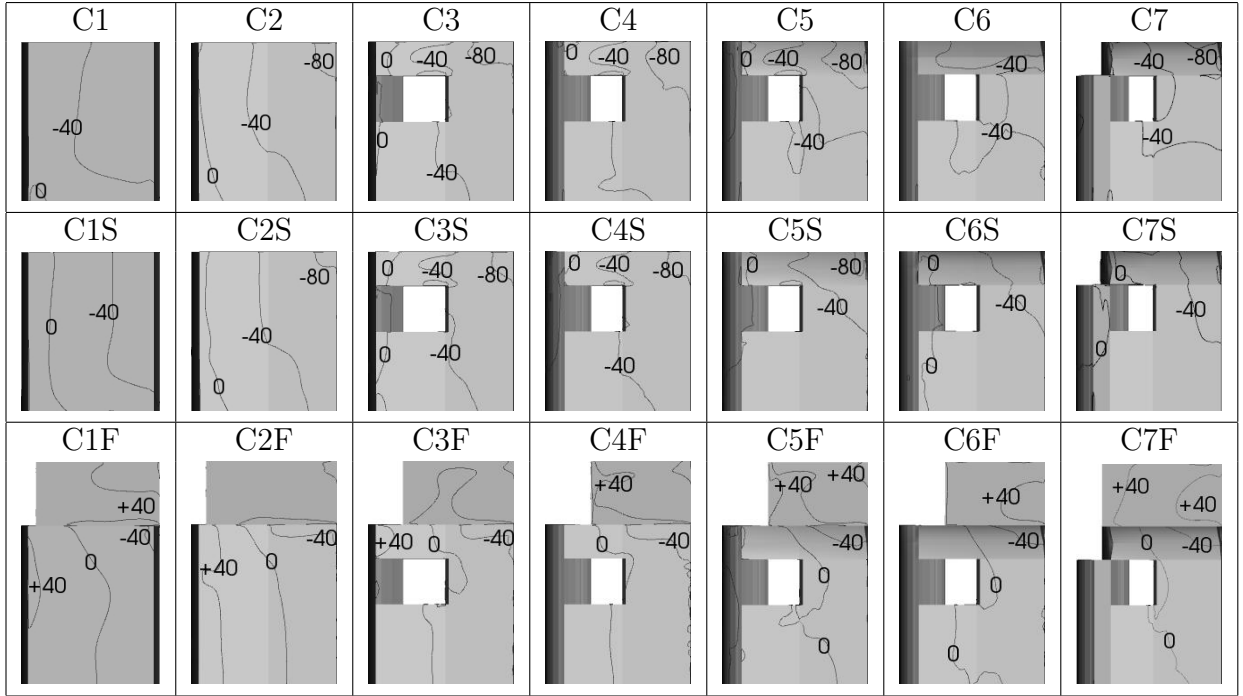


Table 14: Contours of relative static pressure divided by density, $(\frac{p-p_{ref}}{\rho}) [m^2/s^2]$, on the pole suction side

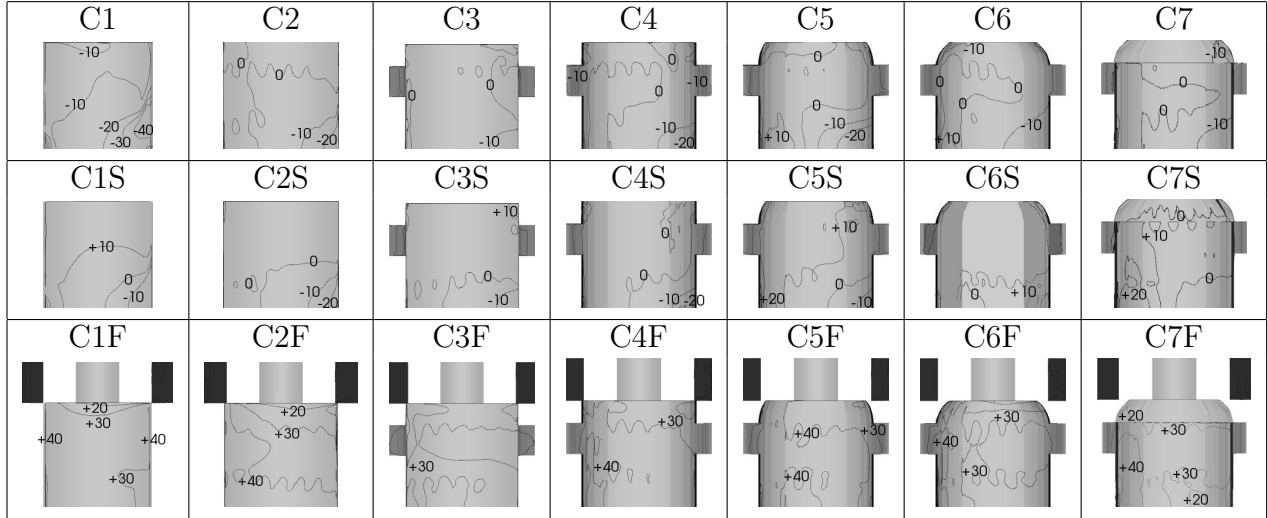


Table 15: Contours of relative static pressure divided by density, $(\frac{p-p_{ref}}{\rho}) [m^2/s^2]$, on the pole front

According to Tables 12-14, near the rotor body there is a region with relatively low $(\frac{p-p_{ref}}{\rho})$ values. This means that the static pressure is low in that region, which causes the air to be sucked stronger into the machine and gives a larger inward velocity near the shaft, c.f. Table 10. The pressure gradients on the rotor body are larger in cases with fan blades in comparison with the base cases. The largest pressure gradients on the rotor body appears in cases with fan blades, which justifies the larger volume flow obtained in those cases.

4 CONCLUSIONS

- Different pole and stator geometries were numerically tested to investigate the cooling air flow through a generator and the results were compared to each other.
- The addition of stator baffles helps to increase the volume flow in the generator and removes the outward velocities at the inlet. The addition of rotor fan blades increases the volume flow in the machine even more.
- The flow separates in the stator channels. The combination of stator baffles and fan blades helps to minimize the separation zone.
- The axial power required by the rotor decreases by using the stator baffles. However, the addition of fan blades increases the required rotor axial power.

5 ACKNOWLEDGEMENTS

The research presented was carried out as a part of the "Swedish Hydropower Centre - SVC". SVC has been established by the Swedish Energy Agency, Elforsk and Svenska

Kraftnät together with Luleå University of Technology, The Royal Institute of Technology, Chalmers University of Technology and Uppsala University, www.svc.nu.

The computational time, hardware and facilities were provided by *c³se*, center for scientific and technical computing at Chalmers University of Technology in Gothenburg Sweden and *SNIC*, Swedish National Infrastructure for Computing.

REFERENCES

- [1] P. Moradnia and H. Nilsson, CFD of air flow in hydro power generators for convective cooling, using OpenFOAM, In proceedings of the *5th European Conference on Computational Fluid Dynamics*, ECCOMAS CFD 2010, J.C.F. Pereira and A. Sequeira (Eds), Portugal, (2010)
- [2] P. Moradnia, CFD of air flow in hydro power generators, Thesis for licenciate of engineering no. 2010:11, ISSN 1652-8565, *Chalmers University of Technology*, Sweden, (2010)
- [3] O. Petit, M. Page, M. Beaudoin and H. Nilsson, The ERCOFTAC centrifugal pump OpenFOAM case-study, *3rd International Meeting of the Workgroup on Cavitation and Dynamic Problems in Hydraulic Machinery and Systems*, Czech Republic, (2009)
- [4] B. E. Launder, B. I. Sharma, Application of the Energy-Dissipation Model of Turbulence to the Calculation of Flow Near a Spinning Disc, *Letters in Heat and Mass Transfer*, **Vol. I, 2**, 131-138 (1974)
- [5] M. Auvinen, J. Ala-Juusela, Nicholas Pedersen and Timo Siikonen, Time-Accurate Turbomachinery Simulations with Open-Source CFD; Flow Analysis Of a Single-Channel Pump with OpenFOAM, In proceedings of the *5th European Conference on Computational Fluid Dynamics*, ECCOMAS CFD 2010, J.C.F. Pereira and A. Sequeira (Eds), Portugal, (2010)